Journal of Sound and Vibration (1997) **204**(2), 239–247

ON THE NON-LINEAR VIBRATION OF THE VON KARMAN SQUARE PLATE BY THE IHB METHOD

A. Y. T. Leung and S. K. Chui

*Department of Mechanical Engineering, University of Manchester M*13 9*PL, U.K.*

(*Received* 9 *November* 1995, *and in final form on* 8 *January* 1997)

Non-linear phenomena in the vibration of a square plate subject to lateral forcing are studied. Starting from the dynamic analogue of the von Kármán partial differential equations that govern the motion of the plate, a system of second order non-linear ordinary differential equations are derived. Using the IHB method, a numerical bifurcation analysis is performed in which interaction between spatial modes is examined. A number of diagrams of resonance curves and bifurcation are presented.

1. INTRODUCTION

Most of the studies of vibrations of thin elastic plates, such as those by Kung and Pao [1], Kisliakov [2] and Pasic and Herrmann [3], are concerned with problems in which only one spatial mode is strongly excited. Sridhar, Mook and Nayfeh [4, 5] and Yang and Sethna [6] represent the motion with more than one mode to consider the effect of internal resonance and the modal interactions. In references [4, 5] the natural frequencies satisfy special relationships, while in reference [6] the equations are solved by the method of averaging. In the present study, we also consider the vibration with two fundamental modes but solve it numerically using the IHB method. Some features of bifurcation are shown to exist in this vibratory problem.

Among model equations for non-linear vibrations of plates, we study those given by Chu and Herrmann [7] which are the dynamic analogue of the von Kármán partial differential equations of the plate. To represent the motion of a thin square plate subject to a symmetrical sinusoidal lateral excitation, two fundamental modes are involved. With the aid of a symbolic computational tool such as Mathematica™, two non-linear ordinary differential equations can be derived through the Galerkin method. Then the IHB method is employed to solve the equations. The stability of the solution is diagnosed using Floquet's theory [8]. For references on the IHB method and stability diagnosis refer to references [9, 10]. One graph of resonance curves (response versus excitation frequency) and two of response curves (response versus excitation force) are presented with some discussion.

2. DERIVATION OF THE SYSTEM OF ORDINARY DIFFERENTIAL EQUATIONS

Consider a flat square plate of thickness h and edge length a. All of the edges are simply supported. The plate are subjected to a lateral excitation force normal to the plate and a constant in-plane stress along the edges. A sketch of the system being studied is shown in Figure 1.

The governing equations of an isotropic plate derived by Chu and Herrmann [7] are

0022–460X/97/270239 + 09 $25.00/0/sv970934

$$u^0_{xx} + d_1 u^0_{yy} + d_2 v^0_{xy} = -w^0_x(w^0_{xx} + d_1 w^0_{yy}) - d_2 w^0_y w^0_{xy},$$

$$v^0_{yy} + d_1 v^0_{xx} + d_2 u^0_{xy} = -w^0_y(w^0_{yy} + d_1 w^0_{xx}) - d_2 w^0_x w^0_{xy},$$

$$D\nabla^4_{xy} W^0 + \rho h w^0_{tt} + 2c w^0_t = q^0 + \frac{Eh}{1-v^2}[(u^0_x + \tfrac{1}{2}w^{0^2}_x)(w^0_{xx} + v w^0_{yy}) + (v^0_y + \tfrac{1}{2}w^{0^2}_y)(w^0_{yy} + v w^o_{xx}) + (1-v) w^0_{xy}(u^0_y + v^0_x + w^0_x w^0_y)],$$

$$\nabla^4_{xy} w^0 = w^0_{xxxx} + 2w^0_{xxyy} + w^0_{yyyy}, \tag{1}$$

where

$$d_1 = \frac{1-v}{2}, \qquad d_2 = \frac{1+v}{2}, \qquad D = \frac{Eh^3}{12(1-v^2)}$$

and the membrane forces are

$$N_x = \frac{Eh}{1-v^2}[u^0_x + v v^0_y + \tfrac{1}{2}(w^{0^2}_x + v w^{0^2}_y)],$$

$$N_y = \frac{Eh}{1-v^2}[v^0_y + v u^0_x + \tfrac{1}{2}(w^{0^2}_y + v w^{0^2}_x)],$$

where u^0 and v^0 are the displacements in the mid-plane of the plate in the x- and y-directions respectively, w^0 is the displacement in the plane normal to the mid-plane and E, v and ρ are the modulus of elasticity, the Poisson ratio and the density, respectively, c is the coefficient of lateral viscous damping and q^0 is the lateral excitation.

We express the governing equations and the membrane forces in the non-dimensional form

$$u_{\zeta\zeta} + d_1 u_{\eta\eta} + d_2 v_{\zeta\eta} = -w_\zeta(w_{\zeta\zeta} + d_1 w_{\eta\eta}) - d_2 w_\eta w_{\zeta\eta}, \tag{2a}$$

$$v_{\eta\eta} + d_1 v_{\zeta\zeta} + d_2 u_{\zeta\eta} = -w_\eta(w_{\eta\eta} + d_1 w_{\zeta\zeta}) - d_2 w_\zeta w_{\zeta\eta}, \tag{2b}$$

$$\nabla^4_{\zeta\eta} w + 4\Omega^2 w_{\tau\tau} + 2\Omega\mu w_\tau = q + 12[(u_\zeta + \tfrac{1}{2}w^2_\zeta)(w_{\zeta\zeta} + v w_{\eta\eta}) + (v_\eta + \tfrac{1}{2}w^2_\eta)(w_{\eta\eta} + v w_{\zeta\zeta}) + (1-v) w_{\zeta\eta}(u_\eta + v_\zeta + w_\zeta w_\eta)], \tag{2c}$$

$$N_\zeta = \frac{\pi^2 Eh^3}{(1-v^2)a^2}[u^0_\zeta + v v^0_\eta + \tfrac{1}{2}(w^{0^2}_\zeta + v w^{0^2}_\eta)],$$

$$N_\eta = \frac{\pi^2 Eh^3}{(1-v^2)a^2}[v^0_\eta + v u^0_\zeta + \tfrac{1}{2}(w^{0^2}_\eta + v w^{0^2}_\zeta)], \tag{3}$$

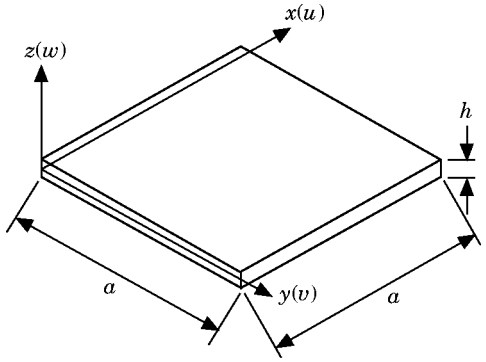

Figure 1. A sketch of the square plate system being studied.

$$\zeta = \pi x/a, \qquad \eta = \pi y/a, \qquad \tau = \omega t,$$

where

$$u^0 = \pi h^2 u/a, \quad v^0 = \pi h^2 v/a, \quad w^0 = hw,$$

$$\omega_0^2 = \frac{\pi^4 E h^2}{3\rho(1-\nu^2)a^4}, \qquad \Omega = \frac{\omega}{\omega_0}, \qquad \mu = \frac{4c}{\rho h \omega_0}, \qquad q = \frac{12(1-\nu^2)q^0 a^4}{\pi^4 E h^4}.$$

We further assume that the lateral load is distributed symmetrically and sinusoidally, so that the related spatial modes are effectively excited. Taking these into account, we choose the first two fundamental orthogonal mode shapes to capture the motion and study their interaction. Thus a solution of w in equations (2) is assumed to be

$$w = z_1 \sin\zeta \sin\eta + z_2 \sin 3\zeta \sin\eta, \qquad z_1 = z_1(\tau), \quad z_2 = z_2(\tau), \tag{4}$$

where z_1 and z_2 are the amplitudes of the modes, say (1–1) and (3–1) respectively and ζ and η range from 0 to π.

Substituting equation (4) into equation (2a, b), u and v can be computed with the aid of a symbolic computational tool, to give

$$\begin{aligned} u = {} & A_1 \sin 2\zeta + A_2 \sin 2\zeta \cos 2\eta + A_3 \sin 4\zeta + A_4 \sin 4\zeta \cos 2\eta \\ & + A_5 \sin 6\zeta + A_6 \sin 6\zeta \cos 2\eta \\ v = {} & A_7 \sin 2\eta + A_8 \cos 2\zeta \sin 2\eta + A_9 \cos 4\zeta \sin 2\eta + A_{10} \cos 6\zeta \sin 2\eta, \end{aligned} \tag{5}$$

where the A_i are the polynomials of z_1 and z_2 listed below:

$$A_1 = z_1\{(\nu-1)z_1 - (6+2\nu)z_2\}/16, \qquad A_2 = z_1(4z_1 + 16z_2 + 8\nu z_2)/64,$$

$$A_3 = (-3+\nu)z_1 z_2/16, \quad A_4 = (19-\nu)z_1 z_2/100, \quad A_5 = (-9+\nu)z_2^2/48, \quad A_6 = 3z_2^2/16,$$

$$A_7 = (-z_1^2 + \nu z_1^2 - z_2^2 + 9\nu z_2^2)/16, \qquad A_8 = z_1(4z_1 - 16z_2 + 8\nu z_2)/64,$$

$$A_9 = (29-\nu)z_1 z_2/200, \qquad A_{10} = z_2^2/16.$$

If constant in-plane stresses N_x and N_y are taken into account, the displacement functions u and v should be modified to be [11]

$$u \to B\zeta + u, \qquad v \to C\eta + v, \tag{6}$$

where B and C are constants to be determined by equation (3) with modified u and v in equation (6) and assumed w in equation (4). Thus we have

$$B = \frac{a^2}{\pi^2 E h^3}(N_x - \nu N_y), \qquad C = \frac{a^2}{\pi^2 E h^3}(N_y - \nu N_x). \tag{7}$$

By substituting the displacement functions given in equations (4) and (6) into equation (2c), and using the Galerkin method, two coupled non-linear second order ordinary differential equations of independent variable τ are obtained, as

$$\begin{aligned} 4\Omega^2 \ddot{z}_1 + 2\Omega\mu\dot{z}_1 + k_1 z_1 + \alpha_{11} z_1^3 + \alpha_{12} z_1 z_2^2 + \alpha_{13} z_1^2 z_2 = q_1(\tau), \\ 4\Omega^2 \ddot{z}_2 + 2\Omega\mu\dot{z}_2 + k_2 z_2 + \alpha_{21} z_2^3 + \alpha_{22} z_1^2 z_2 + \alpha_{23} z_1^3 = q_2(\tau), \end{aligned} \tag{8}$$

where k_i and α_{ij} are given by

$$k_1 = 4 + \frac{12(1-\nu^2)a^2}{\pi^2 E h^3}(N_x + N_y), \qquad \alpha_{11} = \frac{9}{4} + \frac{3\nu}{4} - \frac{3\nu^2}{2},$$

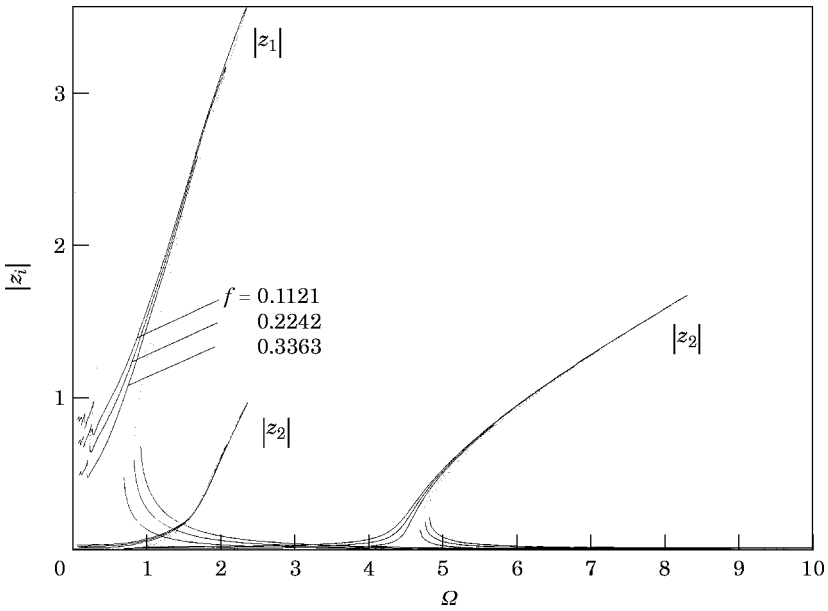

Figure 2. The response $|z_i|$ versus the excitation frequency Ω at three different excitation amplitudes $f = f_1 = f_2$.

$$\alpha_{12} = \frac{753}{100} - \frac{21v}{4} - \frac{630v^2}{50}, \qquad \alpha_{13} = -\frac{45(1-v)}{8} + \frac{9v^2}{4},$$

$$k_2 = 100 + \frac{12(1-v^2)a^2}{\pi^2 Eh^3}(9N_x + N_y), \qquad \alpha_{21} = \frac{369}{4} + \frac{27v}{4} - \frac{123v^2}{2},$$

$$\alpha_{22} = \frac{753}{100} + \frac{51v}{4} - \frac{639v^2}{50}, \qquad \alpha_{23} = -\frac{3}{2} - \frac{3v}{4} + \frac{3v^2}{4},$$

and $q_1(\tau)$ and $q_2(\tau)$ are the amplitudes of the mode $\sin\zeta \sin\eta$ and the mode $\sin 3\zeta \sin\eta$ of the lateral excitation q respectively.

3. SOLVING THE EQUATIONS BY THE INCREMENTAL HARMONIC BALANCE (IHB) METHOD

Among the methods of solving ordinary differential equations, the IHB method is especially effective in evaluating the steady state periodic solution. It is capable of tackling highly non-linear equations. It lends itself to numerical bifurcation analysis, and is a systematic approach in examining bifurcations, such as the fold, the period one bifurcation and the period two bifurcation.

For an excitation of period T acting on the plate, that is, $q(\tau) = q(\tau + T)$, the response is also periodic, since the system now concerned is non-conservative. However, the period of the response may not be T but an integral multiple m of T. Thus we assume the responses in the following form:

$$z_k = \frac{a_k^0}{2} + \sum_{i=1}^{\infty}\left[a_k^i \cos\frac{i\tau}{m} + b_k^i \sin\frac{i\tau}{m}\right], \qquad k = 1, 2.$$

With this assumed solution and using the Galerkin method, the system of ordinary differential equations are discretized into a system of non-linear algebraic equations, and

then linearized using the Newtonian method. Since the solution evaluated by the IHB method is either stable or unstable, a stability checking of the *periodic* solution can be achieved by Floquet's theory [8]. With the aid of the arc-length method [12], the response curves can be traced out in a more systematic manner and several types of bifurcation can be distinguished. The detailed procedure of the IHB method and stability checking are documented in references [9, 10].

4. NUMERICAL EXAMPLE

To examine the vibration behaviour, we take a steel plate as an example. Since in the present study we have only used two modes to represent the displacement w, a qualitative measure of the response is expected. More modes should be taken into account for quantitative results. The parameters of the plate are as follows: density 7850 kg/m^3, modulus of elasticity 200 GPa, Poisson ratio 0·3, coefficient of damping $\mu = 0{\cdot}046$, length 1 m, thickness 0·01 m. We take the two boundary in-plane compressive stresses to be equal, i.e., $N_x = N_y$, and of such value that k_1 equates say, 0·576. For the excitation we consider that $q_1 = f_1 \cos\tau$ and $q_2 = f_2 \cos\tau$, where f_i are force amplitudes. With the parameters defined above, the equations (8) are rewritten as

$$4\Omega^2\ddot{z}_1 + 2\Omega(0{\cdot}046)\dot{z}_1 + 0{\cdot}576z_1 + 2{\cdot}34z_1^3 + 4{\cdot}8048z_1z_2^2 - 3{\cdot}735z_1^2z_2 = f_1\cos\tau,$$

$$4\Omega^2\ddot{z}_2 + 2\Omega(0{\cdot}046)\dot{z}_2 + 82{\cdot}88z_2 + 88{\cdot}74z_2^3 + 10{\cdot}2048z_1^2z_2 - 1{\cdot}6575z_1^3 = f_2\cos\tau. \qquad (9)$$

In equation (9) we take Ω and f to be varying parameters. The results are depicted in Figures 2–4. Figure 2 is a resonance graph of $|z_i|$ against Ω for three different f's, in which $|z_i| = \sqrt{a_0^2/4 + \Sigma a_i^2 + \Sigma b_i^2}$ and $f = f_1 = f_2$. The solid curves represent the stable motion and the dotted curves correspond to the unstable vibration. The points of vertical tangencies at which change of stability occurs are points which give rise to a jump phenomenon

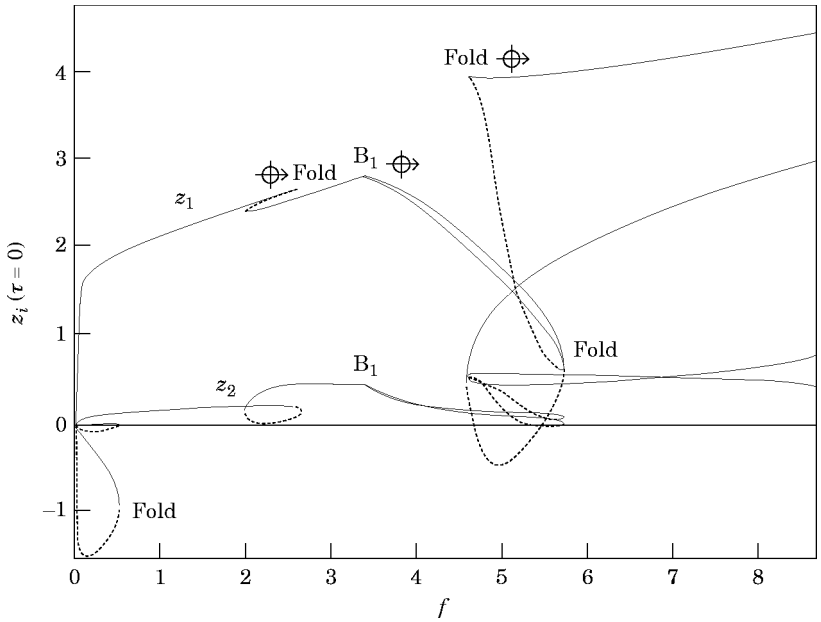

Figure 3. Response $z_i(\tau = 0)$ versus the excitation amplitude $f = f_1$ but $f_2 = 0$ with excitation frequency $\Omega = 1{\cdot}1$.

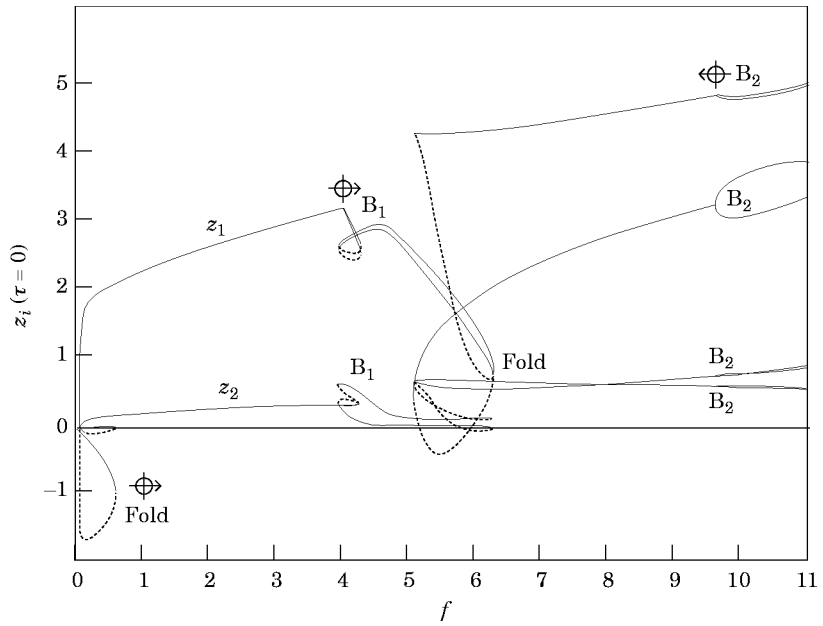

Figure 4. The response $z_i(\tau = 0)$ versus the excitation amplitude $f = f_1$ but $f_2 = 0$ with excitation frequency $\Omega = 1{\cdot}2$.

commonly found in non-linear vibratory elastic systems. According to the terminology suggested by Golubitsky and Schaeffer [13], this is a hysteresis. Within this specified range of f, it can be found that around $\Omega = 2$ the (3–1) mode amplitude z_2 is small when compared with the (1–1) mode amplitude z_1 but is not negligible. Away from $\Omega = 2$ each mode amplitude is dominant over another. From this observation it can be implied that the two mode amplitudes have significant interaction when the excitation frequency is near the fundamental frequency within the specified range of f. Therefore our further investigation will concentrate on the system excited by force with frequency close to the fundamental frequency.

In Figure 2 we have assumed that $f_1 = f_2 = f$, so that both of the spatial modes are excited by their corresponding excitation. Instead of letting $f = f_1 = f_2$, we set $f_1 = f$ and $f_2 = 0$ so as to observe the interaction of the two modes excited by the force of mode (1–1) component only. The results of $z_i(\tau = 0)$ against f are shown in Figures 3 and 4 for a fixed $\Omega = 1{\cdot}1$ and $1{\cdot}2$ respectively. It is observed (Figure 3) that when the force amplitude f is less than $0{\cdot}5$, z_2 is negligibly small. As f increases, there are folds and period one bifurcation, through which the periods of the response remains unchanged. These are indicated on the graph by name: a cross with a unit circle shows the direction in which the eigenvalue of the transformation matrix is escaping unity. For instance, folds and period one bifurcations have an eigenvalue going away from unity with a value of $+1$. To distinguish between these two cases, readers can refer to references [9, 10]. At about $f = 0{\cdot}5$, there is a fold acting significantly on z_1, but not so on z_2, by which z_1 changes from -1 to 2, while a fold at $f = 2{\cdot}5$ affects z_2 more than z_1. Hence, this seems to suggest that both mode amplitudes interact significantly with each other. A further increase in f will produce a period one bifurcation at $f = 3{\cdot}3$ and a fold again at $f = 5{\cdot}5$. One can also note that z_1 increases with f above 8 but z_2 remains more or less constant. In Figure 4 the curves are similar to those in Figure 3 qualitatively, except that the fold at $f = 2{\cdot}5$ vanishes and

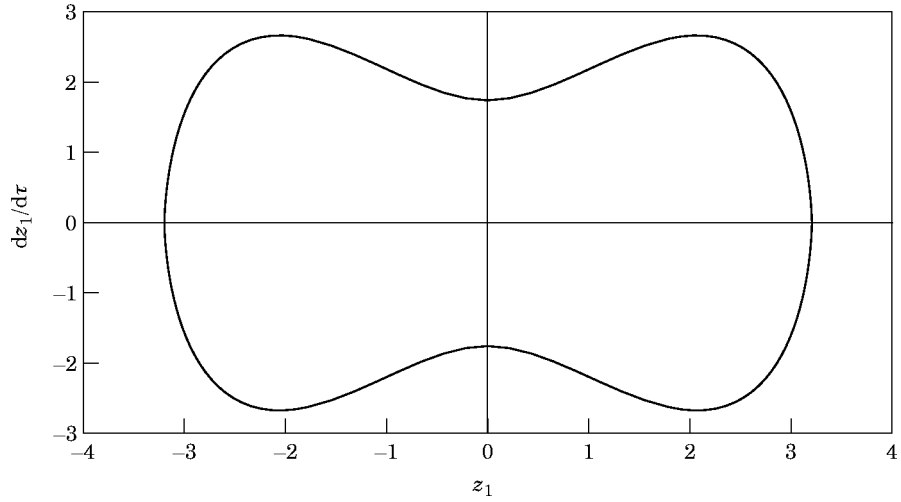

Figure 5. The phase diagram of response z_1 near bifurcation B_1.

a period two bifurcation appears at $F = 9{\cdot}5$, through which not only the magnitude of the response changes but also the period of the response is doubled.

The phase portraits of the system near the bifurcation points in Figure 4 are shown in Figures 5–8 to illustrate its dynamical trajectory. Near bifurcation point B_1, both the response components z_1 and z_2 in Figures 5 and 6 are symmetrical about the origin. Since B_1 is a symmetry breaking point, the symmetry of the phase diagram is preserved before this point, but vanishes after that. The succeeding bifurcation point following B_1 is the period doubling bifurcation point B_2. Two phase diagrams of its response components are delineated in Figures 7 and 8. It is noted easily that the symmetry about the origin of the diagrams has already broken totally, and the shapes are distorted considerably from their corresponding ones in Figures 5 and 6. After this point, the responses of the double period are observed.

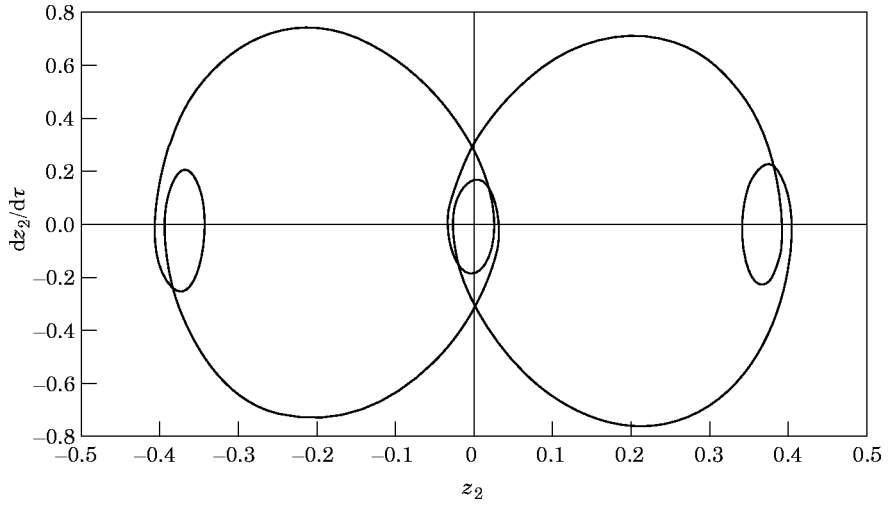

Figure 6. The phase diagram of response z_2 near bifurcation B_1.

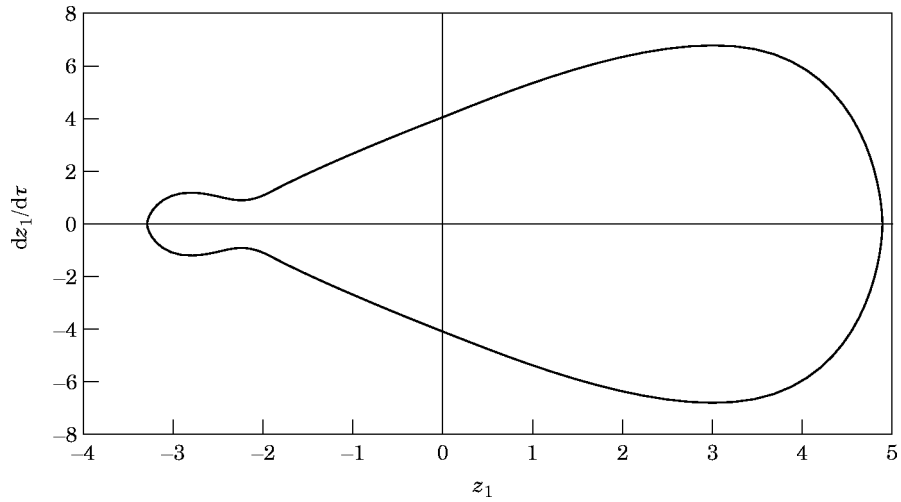

Figure 7. The phase diagram of response z_1 near bifurcation B_2.

If attention is paid only to the interaction between the first two spatial modes being excited dominantly, the Galerkin spatial discretization is inferred to render the modal interaction relation between the modes being considered. Numerical integration methods are then applied to the reliable discretized system. The same results as those of the IHB method are obtained within the excitation range. It is evident that the results from the IHB method can reveal the actual behaviour of the system provided that the Galerkin method is appropriate for the spatial discretization.

5. CONCLUDING REMARKS

With the use of the Galerkin method and the IHB method, the vibration phenomena of a thin square plate governed by von Kármán equations are investigated. More than one spatial mode to fit the motion is involved, so that modal interactions are taken into account

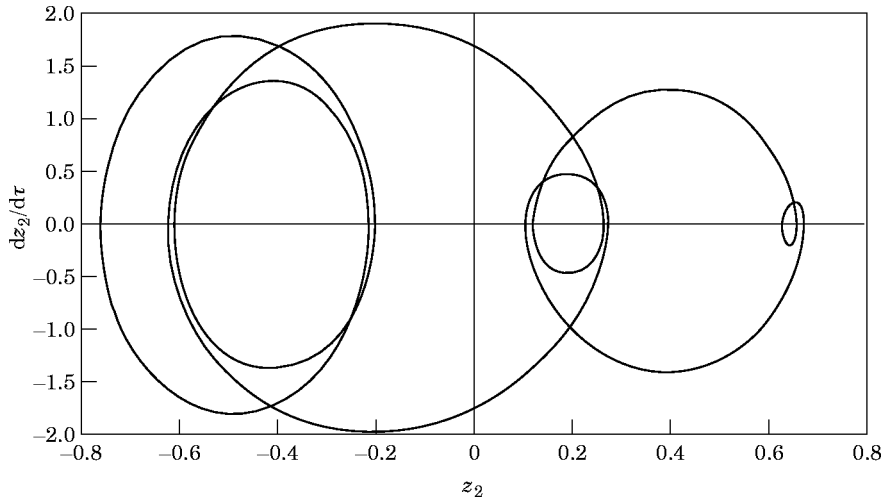

Figure 8. The phase diagram of response z_2 near bifurcation B_2.

qualitatively. Cases in which one mode or both are excited strongly are considered. Especially in the former case although only the fundamental mode is motivated, both mode amplitudes are excited considerably, and significant modal interaction and bifurcation features are discerned. Further research could be undertaken to consider the vibration of a rectangular plate with many spatial modes to capture the motion.

REFERENCES

1. G. C. Kung and Y. H. Pao 1972 *Journal of Sound and Vibration* **39**, 1050–1054. Non-linear flexural vibrations of a champed circular plate.
2. S. D. Kisliakov 1976 *International Journal of Non-linear Mechanics* **11**, 219–228. On the non-linear dynamic stability problem for thin elastic plates.
3. H. Pasic and G. Herrmann 1984 *Journal of Sound and Vibration* **95**, 469–478. Effect of in-plane inertia on the buckling of imperfect plates with large deformations.
4. S. Sridhar, D. T. Mook and A. H. Nayfeh 1975 *Journal of Sound and Vibration* **41**, 359–373. Non-linear resonances in the forced responses of plates, part I: Symmetric responses of circular plates.
5. S. Sridhar, D. T. Mook and A. H. Nayfeh 1978 *Journal of Sound and Vibration* **59**, 159–170. Non-linear resonances in the forced responses of plates, part II: Asymmetric responses of circular plates.
6. X. L. Yang and P. R. Sethna 1990 *Journal of Sound and Vibration* **155**, 413–442. Non-linear phenomena in forced vibrations of a nearly square plate: antisymmetric case.
7. H. Chu and G. Herrmann 1956 *Journal of Applied Mechanics* **23**, 523–540. Influence of large amplitudes in free flexural vibrations of rectangular elastic plates.
8. J. A. Richards 1983 *Analysis of Periodically Time-varying Systems*. New York: Springer-Verlag.
9. A. Y. T. Leung and T. C. Fung 1989 *Journal of Sound and Vibration* **131**, 445–455. Construction of chaotic regions.
10. A. Y. T. Leung and S. K. Chui 1995 *Journal of Sound and Vibration* **181**, 619–633. Non-linear vibration of a coupled Duffing oscillator by an improved incremental harmonic balance method.
11. D. J. Dawe, S. S. E. Lam and Z. G. Azizian 1993 *Computers & Structures* **48**, 1011–1023. Finite strip post-local-buckling analysis of composite prismatic plate structures.
12. R. Seydel 1988 *From Equilibrium to Chaos*. New York: Elsevier.
13. M. Golubitsky and D. G. Schaeffer 1985 *Singularities and Groups in Bifurcation Theory*, *Volume 1*, New York: Springer-Verlag.